Chapter

Wavelet Transform Applied to Internal Defect Detection by Means of Laser Ultrasound

Hossam Selim, Fernando Piñal Moctezuma, Miguel Delgado Prieto, José Francisco Trull, Luis Romeral Martínez and Crina Cojocaru

Abstract

Laser-generated ultrasound represents an interesting nondestructive testing technique that is being investigated in the last years as performative alternative to classical ultrasonic-based approaches. The greatest difficulty in analyzing the acoustic emission response is that an in-depth knowledge of how acoustic waves propagate through the tested composite is required. In this regard, different signal processing approaches are being applied in order to assess the significance of features extracted from the resulting analysis. In this study, the detection capabilities of internal defects in a metallic sample are proposed to be studied by means of the time-frequency analysis of the ultrasonic waves resulting from laser-induced thermal mechanism. In the proposed study, the use of the wavelet transform considering different wavelet variants is considered due to its multi-resolution time-frequency characteristics. Also, a significant time-frequency technique widely applied in other fields of research is applied, the synchrosqueezed transform.

Keywords: laser ultrasound, internal defect detection, wavelet transform, synchrosqueezed transform, time of flight, nondestructive testing

1. Introduction

Structural damage is a typical defect in metallic structures and components that are exposed to deformations during the manufacturing process. Such undesired physical discontinuities imply quality level affectation of the final products and even the posterior performances when subjected to complex and cyclic loadings during their service. Thus, in the last years, a more comprehensive attention has been taken to nondestructive testing (NDT) methods in order to inspect the internal characteristics of metallic components for looking for internal defects or discontinuities.

In this regard, the use of conventional Acoustic Emission (AE) transducers has the advantages of moderate cost and easy implementation, and it allows the generation of specific waveforms with a known pulse shape. Although these methods provide satisfactory results, AE transducers also show some drawbacks including the low output power, that prevents such systems from being used remotely, low frequency bandwidth range, that makes necessary the use of arrays or ultrasonic

scanners increasing the system overall cost, small surface area, that prevents covering large object areas at once, and low spatial resolution in the excited volume. Ultrasonic transducers use waves with central frequencies ranging from fractions to multiples of MHz. AE analysis commonly relies on either of two schemes, pulse-echo mode or pitch-catch mode. Pulse-echo mode is more useful in applications where it is required to use only one sensor for the send/receive signals. This has some limitations on some data acquisition speed and sensor's sensitivity and size. It is also hard to recognize the location of the defects at an angle. Hence, the defect should be vertically aligned with the sensor in order to catch it. The pitch-catch mode offers more flexibility to work in both transmission and reflection modes where it is possible to more deeply investigate the ultrasonic-material interaction at different levels inside the material and extract more data concerning the defect by taking measurements at different angles. However, this technique is more expensive as it requires the use of many sensors, and the data processing is slower [1–3]. The frequency of the ultrasonic signal used affects the sensitivity and resolution of the measured defect dimensions. At higher frequencies, smaller defects can be detected more accurately. However, increasing the frequency has a negative impact on wave propagation inside the material. In other words, higher frequencies travel closer to the surface. So, the portion of the waves that penetrate to the depth of the material is reduced, thus leading to weaker possibilities to catch deeply embedded defects. Most of the available ultrasonic NDT instruments use these types of conventional AE transducers. Typically, they analyze the ultrasonic pulse's Time of Flight (TOF) through the material under test (from the transducer to the receiver) in order to identify discontinuities in the structure corresponding to potential defects.

As an alternative, photonic approaches based on laser-induced ultrasonic and optical detection showed up as valuable competitors to the conventional ultrasonic techniques in the NDT field. These techniques offer the possibility of remote transmission and detection at a much higher resolution [4, 5]. The energy carried by a laser pulse incident on an isotropic specimen is rapidly absorbed into a shallow volume of the material and creates a localized heating, which results in a thermo-elastic expansion of the material, inducing a stress wave that generates an acoustic pulse [2]. Such thermoelastic effect plays an important role in ultrasonic wave generation when the power density of the pulsed laser is lower than the ablation threshold of material. Ultrasonic waves mainly include longitudinal waves, shear waves, surface acoustic waves, and Lamb waves. Optical systems based on the laser technology can be used as well for the detection of transmitted and/or reflected acoustic waves. Several methods are implemented for this purpose. The vibration created by the acoustic wave at the surface can be optically detected using several approaches. They include optical interference techniques where a laser beam, reflected by the object surface, interferes with a reference beam. The interference fringes provide information about the crack's position and size. A Mach-Zehnder interferometer is the simplest example for how interference fringes are generated. The holographic interferometry technique is most commonly used for crack localization and flaw size determination [6]. It can detect very small details of the object under test. The optical approaches have important advantages such as the remote noncontact application, remote control, and generation of broadband frequency waves from kHz to GHz, high output power and the possibility to easily scan a larger object area at once. As an example of this performance, the work presented by Zhao et al. used this method for fatigue and subsurface crack detection [7]. Also, Erdahl discussed a valuable example of this approach to inspect multi-layered ceramic capacitors [8]. The main drawbacks of optical detection methods are their critical stability and the need for an anti-vibration setup in order to obtain reliable results, which make them very expensive and hard to apply to certain related fields. On the other side, it

is difficult to control the acoustic pulse shape as this mainly depends on the optical beam absorption properties at the material surface.

In this regard, a third approach represented by a hybrid scheme, composed by laser-ultrasonics, is considered a good trade-off in order to take advantage of both strategies, that is, the advantages of the optical system for generating artificial acoustic emission waves, as well as using a conventional ultrasonic transducer for detection. This significantly shows interesting results that overcome the drawback of the other schemes. Laser-ultrasonics offers an alternative to conventional ultrasonic techniques in the field of NDT evaluation. It allows inspection at a far distance from the object allowing the remote investigation of the test specimen without the need for a direct contact. Additionally, this technique features a broader frequency bandwidth compared with the limited bandwidth of the conventional ultrasonic transducers. Practically speaking, laser-ultrasonics covers the majority of the ultrasonic bandwidth which is important for various applications involving material characterization [2]. Indeed, the potential of this hybrid sensing scheme, combined with performative signal processing techniques, results in a promising field of study. Many researchers have made efforts to investigate the features of laser-generated acoustic waves and got substantial research achievements. For example, Zhang et al. studied empirical mode decomposition (EMD) to analyze the ultrasonic signals captured from an object that suffers from a certain defect which is followed by the Fourier transform of the selected intrinsic mode functions (IMFs) extracted from the EMD [9]. Also, Li et al. studied the laser-generated ultrasonic wave frequency characteristics in order to analyze crack effects and extract them from their generated frequency components [2]. Dixon et al. used pulsed laser-generated ultrasonics and EMAT for detecting the crack position using the B-scan study in time and frequency domains [10]. Lee discussed the ultrasonic flaw signal and technique to extract features using the fast Fourier transform and discrete wavelet transform [11]. All these studies conclude that broadband frequency components appear in the ultrasonic waves generated by the laser impulse. The Fourier Transform (FT) is the simplest and most straight forward topology for separating the frequency's components and studying their responses individually. However, it has some drawbacks since it does not allow the visualization of the temporal fingerprints of those individual frequencies. This makes it harder to figure out which frequency component corresponds to the defect. That necessitates the use of a stronger technique as the Wavelet Transform (WT) in order to analyze these frequency components and extract only those that correspond to the defect under investigation. Thus, the WT shows what frequencies are present and their impact on the time domain. Hence, it is possible to distinguish temporal and spectral behaviors, both at a time. This property helps to get more specific information about the TOF of possible reflected signals from the material with defects. Higher frequencies travel faster and closer to the surface of the object under test, compared with the lower frequencies. The wavelet technique helps to visualize the propagated frequencies at certain time instants in the ultrasonic signal life time.

Considering the nature of the acoustic emission waves generated by the laser excitation, the detection of the TOF represents a challenge that is being currently attended to by the scientific community [12]. Although some studies have exhibited the potential of the WT to analyze acoustic emission signals, the analysis and interpretation of the resulting time-frequency maps under a laser-ultrasonic scheme is still a challenge, mainly with respect to the determination of the TOF, where the error minimization is highly important. In fact, the error in determining the TOF, due to the presence of defects in the material under inspection, could become a challenge due to inconsistencies in the analysis. In this regard, the wavelet transform capabilities and some of the most recent variants exported from other fields of

investigation, as the Synchrosqueezed Transform (ST), are considered. Thus, in this chapter, a defective metallic component for damage detection and visualization, through a laser-ultrasonic approach and detection of AE waves TOF, is studied. For this objective, the wavelet transform performance, as a time-frequency processing tool, and its results, are studied, compared with a promising variant called synchrosqueezed transform. This chapter is organized as follows: The theoretical basis and its suitability for the ultrasound processing of the wavelet transform and the synchrosqueezed transform are presented in Section 2. The materials and method, including the experimental setup, are explained in Section 3. The competency of the techniques and the experimental results are presented and discussed in Section 4. Finally, this chapter shows the conclusion dissemination in Section 5.

2. Theoretical considerations

2.1 Wavelet transform

The conventional Fourier series representation gives the information of frequency components in a periodic signal (inability to provide frequency information over a period of time). The simplest solution, then, is to apply the FT within a limited time interval. Thus, the time window is shifted, and frequency components are obtained using the FT. This is the principal idea of the Short Time Fourier Transform (STFT). However, due to its fixed time window, its capabilities in front of complex nonstationary signals, where frequency components vary widely over a short time interval, are reduced. The wavelet transform overcomes such limitations by introducing a scaling function, which gives a variable time window. The WT provides a variable frequency resolution unlike the FT and STFT which have a constant resolution [13].

The selection of the mother wavelet provides different characteristics of the input signal set that can emphasize certain features at the output. The flexibility of choosing the optimal mother wavelet is one of the advantages of using the WT, since the choice of the mother wavelet for a particular problem improves the signal processing capability of the technique. If the shape of the signal to be detected is known a priori, a replica of the set can be utilized as the mother wavelet function, or the mother wavelet can be chosen from a set of theoretical signals. The Mexican hat, Morlet and Daubechies4 (db4) wavelets have been proven to be efficient in improving the signal strength and reducing the noise, making the WT-based technique extremely useful for flaw detection (**Figure 1**).

The wavelet transform employs a sliding window function that is used to decompose the signal into a sum of wavelets added together. Each wavelet has finite propagation in time determined by the window size. These wavelets are limited in time, whereas sinusoidal functions, which are used for the Fourier series and Fourier transform, are continuous in the whole time range. Hence, we can use these wavelets

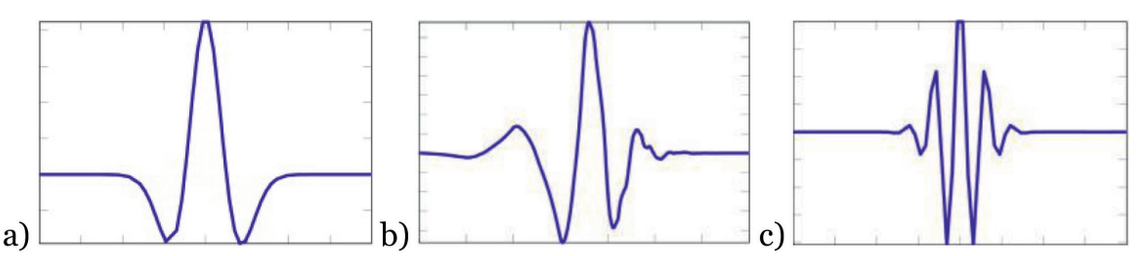

Figure 1.
Examples of wavelets used for acoustic emission processing. (a) Mexican hat. (b) Daubechies. (c) Morlet.

that can be stretched/compressed in frequency and shifted in time to correlate them with the original signal under analysis in order to determine the set of frequencies propagating at any instantaneous time to a certain level of accuracy that is still not completely accurate due to the uncertainty principle, but this accuracy is sufficient to acquire enough information about both time and frequency composition of the signal.

Assuming that a multicomponent time series signal of interest $v(t)$ can be expressed in the general form (Eq. 1):

$$v(t) = \sum_{k=1}^{K} a_k(t)\exp\cos(2\pi i\,\phi_k(t)) \tag{1}$$

where $a_k(t)$ are the time-dependent instantaneous amplitudes, $\phi_k(t)$ denotes the instantaneous phases, and consequently, $\phi'_k(t)$ represents its instantaneous frequencies. The wavelet transform can be represented Eq. (2), where the wavelet transform Wv from the $v(t)$ signal is obtained:

$$W_v(a,b) = \frac{1}{\sqrt{|a|}}\int_{-\infty}^{\infty} v(t)\,\psi^*\left(\frac{t-b}{a}\right)dt \tag{2}$$

where ψ^* is the complex conjugation of the mother wavelet (a continuous function in both the time domain and the frequency domain). A scale factor a either stretches (a is large), or compresses (a is small) the signal, where a = $\omega o_{/}\omega$, ω is the angular frequency and ω_o is the angular frequency shift, while b is the signal's time shift [14–16]. The main purpose of the mother wavelet is to provide a source function to generate the daughter wavelets which are simply the translated and scaled versions of the mother wavelet.

2.2 Synchrosqueezed transform

Although, in comparison with the time-dependent Fourier transform (i.e., STFT), the achieved resolution of the time-frequency representation (TFR) by means of the wavelet analysis is certainly improved, its use still entails uncertainties on the distribution of energy for the said representation. This becomes particularly evident for nonstationary signals with a higher multimodal complexity. While it is true that these inaccuracies somehow respond to the Heisenberg-Gabor uncertainty principle [17], the fact is that they are heavily related to the choice of the wavelet function with regard to the phenomenon of the application.

In order to overcome this drawback, alternative TFR strategies have been developed. As is the case of the Wigner-Ville distribution (and their modified alternatives, e.g., Gabor-Wigner, Choi-Williams, Cohen's class, Zhao-Atlas marks, among others), despite accomplishing high resolution TFRs, their use results in additional difficulties as in the case of high computational load and artificial frequency components due to the interference between actual ones (cross-term property).

An additional TFR technique is the Hilbert-Huang Transform (HHT); by means of an Empirical Mode Decomposition (EMD) of the analyzed signal, a collection of Intrinsic Mode Functions (IMFs) is obtained, which, along with the Hilbert spectral analysis, will lead to a time-frequency depiction. Although having been successfully applied in a wide range of fields due to adaptively decomposing the signal of interest, its use also carries some drawbacks. Such is the case of a high computation load, the requirement of a stopping criterion for the EMD, the difficulty for discerning separate frequency components in narrow-band signals and a mix of modal components.

A more recent TFR framework inspired, by the adaptive approach of the HHT and the redistribution concept of the Wigner-class analysis, is the Synchrosqueezing

Transform (ST). This framework was developed with the aim to eliminate distorted interference terms while concentrating the energy on their corresponding modal components. This method, belonging to the family of the time-frequency energy reassignment, has arisen with the advantages of offering a better adaptability with regard to the signal, lesser deformation for the IF profiles, and by preserving the time, it admits an exact reconstruction formula for the constituent modal components (i.e., existence of an inverse transformation). Originally proposed for Daubechies [18] for an auditory application and revised for several authors [19–23], it works by redistributing the misallocated energy on the scale axis (due to the mother wavelet).

As aforementioned, the wavelet analysis leads to a depiction of the instantaneous frequencies $\phi'_k(t)$ of each existing component in the signal $v(t)$ by a correlation between said signal and a chosen atom (mother-wavelet), thus using a scaled and translated version of the mother-wavelet over $v(t)$. Nevertheless, under this framework is presented energy spreading over the TFR associated due to the selection of the mother-wavelet as well as for the Heisenberg-Gabor uncertainty principle, affecting the intelligibility of the analysis. The aim of the synchrosqueezed wavelet transform is to partially reassign the spread energy that occurred during the wavelet analysis for the frequency dimension only, by analyzing each component of the TFR. Therefore, it is necessary that the modal components are intrinsic mode type functions (IMT). Hence, by preserving the time dimension, it is possible to enable an inverse transformation of the obtained signal toward a time series. The wavelet synchrosqueezed transform (WST) involves the following steps. First, obtaining a wavelet transform Wv from the $v(t)$ signal following Eq. (2). Thus, ψ represents the analytic mother wavelet existing only for positive frequencies, that is, the Fourier transform of the mother-wavelet $F_{[\psi]}$ given by:

$$\hat{\psi}(\xi) = \frac{1}{2\pi\sqrt{a}}\int_{-\infty}^{\infty}\psi(t)\,\exp(-i\xi t)dt = 0 \tag{3}$$

for frequencies $\xi < 0$. By Plancherel's theorem, Eq. 2 can be rewritten as:

$$W_v(a,b) = \frac{1}{2\pi\sqrt{a}}\int_{-\infty}^{\infty}\hat{v}(\xi)\,\hat{\psi}^*(a\xi)\,\exp(ib\xi)d\xi = \frac{A}{4\pi\sqrt{a}}\hat{\psi}^*(a\,\omega_0)\,\exp(ib\,\omega_0) \tag{4}$$

where $\omega_0 = 2\pi f_0$ is the angular frequency of $v(t)$.

Second, extracting the IF from the wavelet transform. As each scale a of Eq. (5) corresponds to a natural frequency ξ/ω_0, satisfying the relation $a = c/\xi$ where c is the center frequency of the mother-wavelet ψ^*; it concentrates the energy of the transformation around this frequency. By supposing that the shift time b is fixed, and if $\xi = c/a$ is close, but not exactly located at the instantaneous frequency $\phi'_k(t)$, the coefficient $W_v(a,b)$ will contain some residual nonzero energy (i.e., $|Wv(a,b)|^2 > 0$), smearing the TFR. The aim of the synchrosqueezing is to remove this residual energy centered around ξ and reallocating it to a frequency location closer to its corresponding instantaneous frequency $\phi'_k(t)$. So, it is necessary to compute the instantaneous frequency of the wavelet analysis for which $W_v(a,b) \neq 0$, by the phase transformation:

$$\omega_v(a,b) = \frac{1}{i\,W_v(a,b)}\frac{\partial(W_v(a,b))}{\partial b} \tag{5}$$

Third, "squeezing" the wavelet transform over the regions where the phase transformation is constant.

During the scale-frequency mapping, that is, $(a,b) \rightarrow (\omega_v(a,b),b)$, the synchrosqueezing is applied to reassign the time-scale representation of the TF. Thus, for a fixed shift time b, the frequency reassignment $\omega_v(a,b)$ is carried out for all a scale

values by means of Eq. (5), to then, for each frequency of interest ω_l, compute the synchrosqueezing by adding all values $W_v(a,b)$, where the reassigned frequency $\omega_v(a,b)$ is equal to ω_l. This is achieved by means of the mapping (for discrete values):

$$T_v(\omega_l, b) = \frac{1}{\Delta\omega} \sum_{a_k:\left|\omega(a_k,b)-\omega_l\right| \le \frac{\Delta\omega}{2}} W_v(a_k, b)\, a_k^{-3/2} (\Delta a)_k \tag{6}$$

where $\Delta\omega = \omega_l - \omega_{(l-1)}$, $(\Delta a)_k = a_k - a_{(k-1)}$, ω_l is the lth discrete angular frequency, and a_k is the kth discrete scale point. Finally, the instantaneous angular frequency can be normalized by 2π as the IF $f = \omega/2\pi$.

In general, the modal components from the synchrosqueezed analysis are separated well enough in the TF plane. For a given signal, if this condition is actually met, their modal components could be treated as intrinsic mode function types and their trajectories (known as wavelet ridges) can be tracked over the TF plane as their energy varies in terms of the function of time, enabling their transformation into the time domain.

3. Method and material

In order to analyze the suitability of the wavelet transform and the synchrosqueezing to extract a proper TOF related to defect location, a specific experimental bench has been arranged. The procedure is based on five steps. The first step consists of the caption of the ultrasonic signals received by the ultrasonic sensors from all considered laser scan points. These acquired signals are then processed by a noise filtering algorithm and an interpolation and bandpass filter to remove any unimportant components. The resulting A-scan signals are then ready for the next step of applying the wavelet or the synchrosqueezed transform. These transforms will generate the time frequency maps that are useful for detecting the most important propagating frequencies with respect to their times of flight. In order to further clean the signal, it is proposed to apply a signal contouring algorithm. This will help to identify the areas with uniform intensities, and the signal distribution will become clearer. It should be noted that the most important feature in this kind of algorithm is the expected time of flight for the signal. This time of flight is used later on detecting the distance between the sensor and the defect based on the speed of propagation of the ultrasonic waves (**Figure 2**).

The distance between the individual laser scan points and the receiving sensor is known a priori. In addition, the dimensions of the object under test are also known. In this regard, the time of flight of the main echoes should be equal to, or greater than, either the distance of the path from the laser direct to the sensor, or from the laser to any object boundary and reflecting back to the sensor whichever found shorter. Thus, the distance between the laser and the object boundaries is larger than the direct distance between the laser and the sensor. In addition, if there is any existing defect inside the material, this would create an internal deflection with a distance shorter than that of the object's boundaries. Hence, it is expected that the first main echo received in the analysis is due to the laser's direct propagation toward the sensor, and the second main echo, in this case, should be due to the deflections from any existing defect.

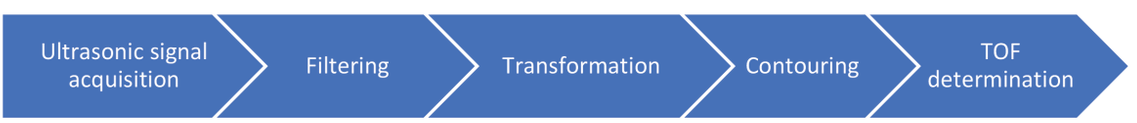

Figure 2.
The sequence flow chart of the signal processing procedure for the analysis.

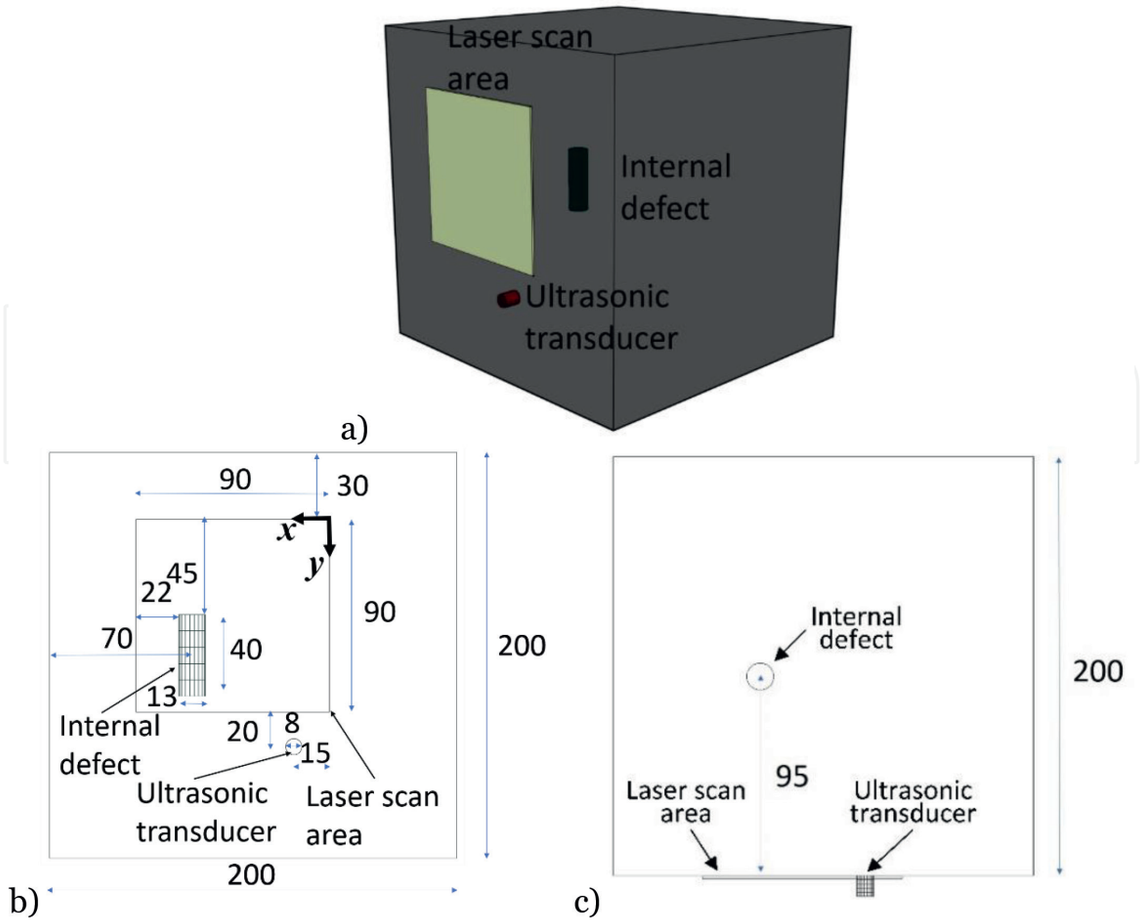

Figure 3.
Aluminum specimen, internal damage, and laser scan area. All dimensions are in millimeters. (a) Isometric view. (b) Front view. (c) Top view.

The TOF corresponding to the presence of the defect will be equal to the sum of TOF from source of excitation to the defect scatterer and the TOF from the defect scatterer to the receiving sensor. IF this TOF is converted to distance by multiplying by the longitudinal velocity of sound in the material, we can see that the position of the defect scatter would be any point at the surface of a locus ellipsoid whose two foci are the exciter and sensor positions [24].

An aluminum cube, with dimensions of 200 mm^3, and with an embedded cylindrical defect is considered to investigate the detection capabilities of the wavelet and synchrosqueezed transforms. The sample's structure and the position of the defect are shown in the next figure. The hole under investigation is the one on the top around the scan area of the laser-generated ultrasound (**Figure 3**).

4. Experimental results

This section shows the wavelet analysis of each A-scan signals detected by the sensor at positions indicated in **Table 1**. Three different types of mother wavelets are used to analyze the signal, namely the Mexican hat, Morlet, and db4. The three mother wavelets are very popular for ultrasound wave analysis due to their high correlation with the ultrasound wave form.

Figure 4 shows the cross section front view at XY plane of the cylindrical defect embedded at depth of the object. The position of the three scan points at the surface of the object are superimposed on same Figure for clarification the horizontal and

Scan point	*X* position	*Y* position	True time of flight
R1	11	51	19.65
2	31	51	18.30
3	81	51	17.10

Table 1.
Scan points considered for samples inspection.

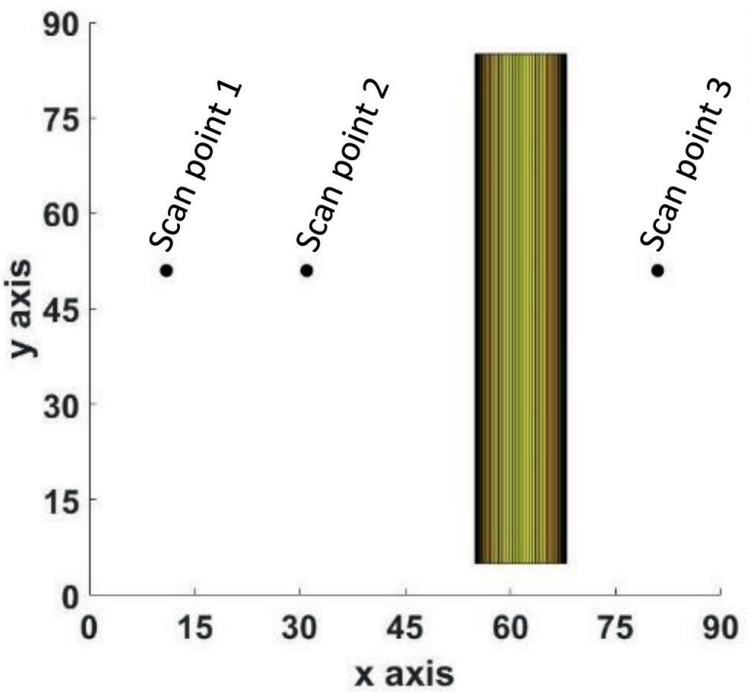

Figure 4.
Scan points considered for sample inspection and synthetic defect location.

vertical spacing from cylindrical defect. The exact data of the position of each scan point is represented in **Table 1**.

Figure 5 shows the absolute position of the defect cylinder represented by top view for the three scanning points. In addition, the locus ellipsoid estimation based on distance corresponding to TOF from exciter to defect point scatter and back to the receiving sensor for the three scanning points. It can be seen that the intersection between the ellipsoid and the cylinder happens at the point of back scattering from the defect to the sensor.

It is shown in **Figure 6** the wavelet contour map generated using Morlet WT. It is clear that the WT analysis resulted in clustering the signal into groups of segregated echoes. Each echo is governed by its intensity level, time duration, and scale levels. Scale levels are inversely proportional to the frequency spectrum. Hence, we can see at the top of the WT spectrum lies the echoes with low frequencies, while the echoes at the bottom correspond to high frequency components. Each of these echoes starts at a certain time shift, and it is clear that the start of the echo is occurring at lower frequencies with less intensity, and later the higher frequency components start to appear with their intensity level increasing. TOF of the first echo is corresponding to the direct surface propagation of the signal from the excitation point to the receiving sensor position, while TOF of the second large echo signal is corresponding to the reflected signal from the defect. It is possible to estimate the corresponding TOF based on that conclusion to be 20, 19, and 18.5 μs

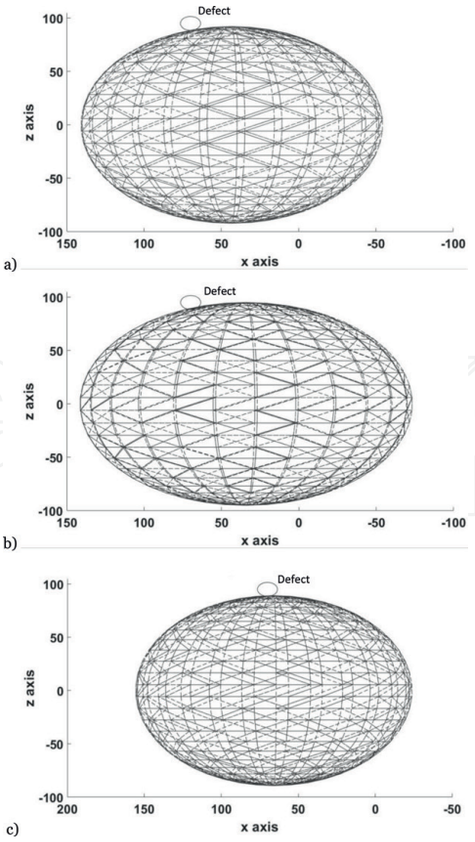

Figure 5.
Ellipsoid locus of defect position based on true time of Flight estimation resulting from the scan point and acoustic transducer positions. (a) Scan point 1. (b) Scan point 2. (c) Scan point 3.

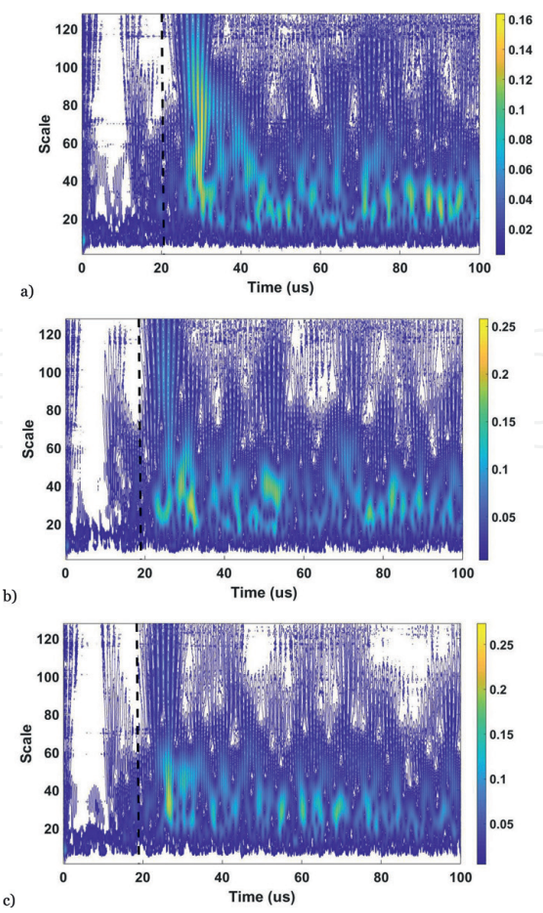

Figure 6.
Resulting wavelet contour maps with Morlet wavelet. (a) Scan point 1. (b) Scan point 2. (c) Scan point 3.

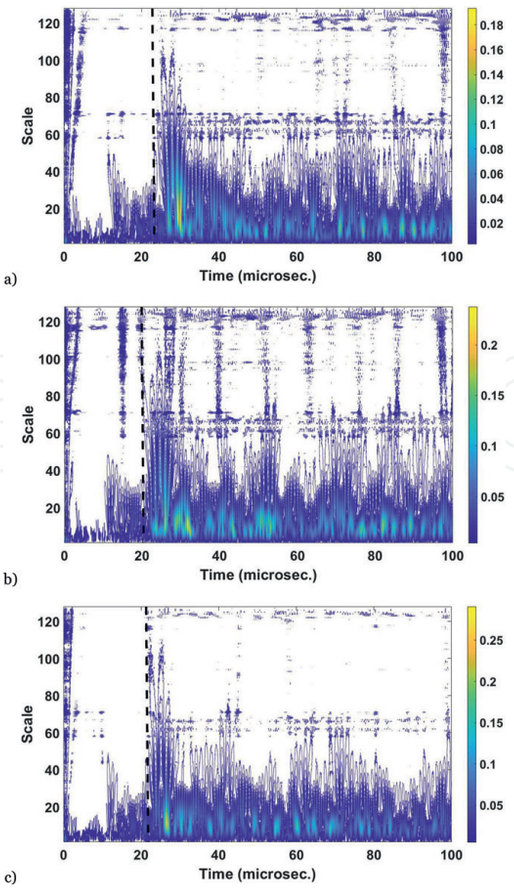

Figure 7.
Resulting wavelet contour maps with Mexican hat wavelet. (a) Scan point 1. (b) Scan point 2. (c) Scan point 3.

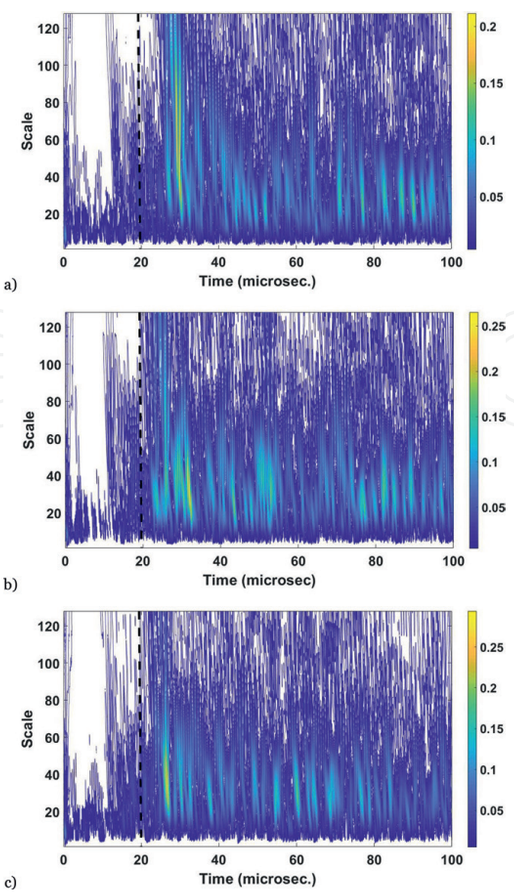

Figure 8.
Resulting wavelet contour maps with db24 wavelet. (a) Scan point 1. (b) Scan point 2. (c) Scan point 3.

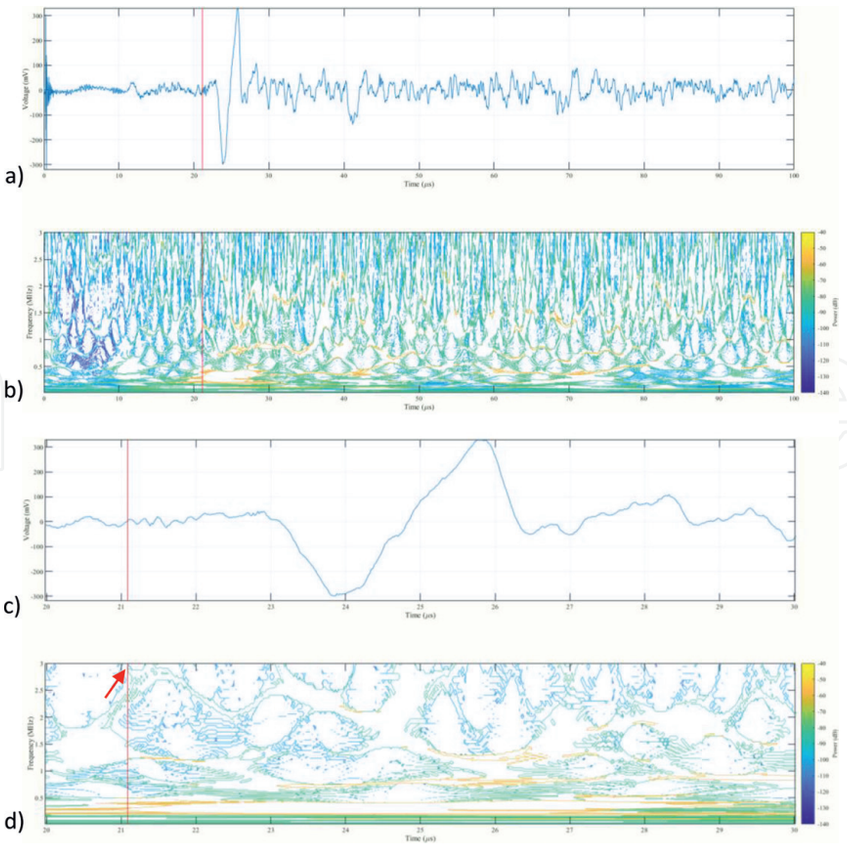

Figure 9.
Synchrosqueezing wavelet transform contour map of the scan point 1. (a) Time-based signal. (b) Synchrosqueezing transform contour map. (c) Detail of the time-based signal. (d) Detail of the synchrosqueezing transform contour map with an initial presence of acoustic activity at 21.08 μs, 2.87 MHz @−80.31 dB.

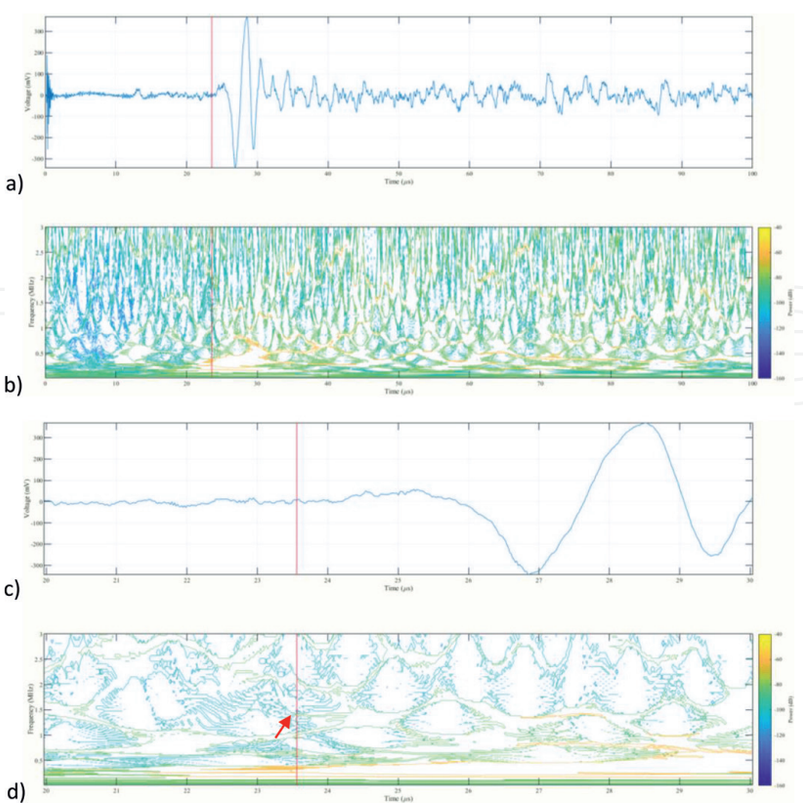

Figure 10.
Synchrosqueezing wavelet transform contour map of the scan point 2. (a) Time-based signal. (b) Synchrosqueezing transform contour map. (c) Detail of the time-based signal. (d) Detail of the synchrosqueezing transform contour map with an initial presence of acoustic activity at 23.56 μs, 2.15 MHz @−84.04 dB.

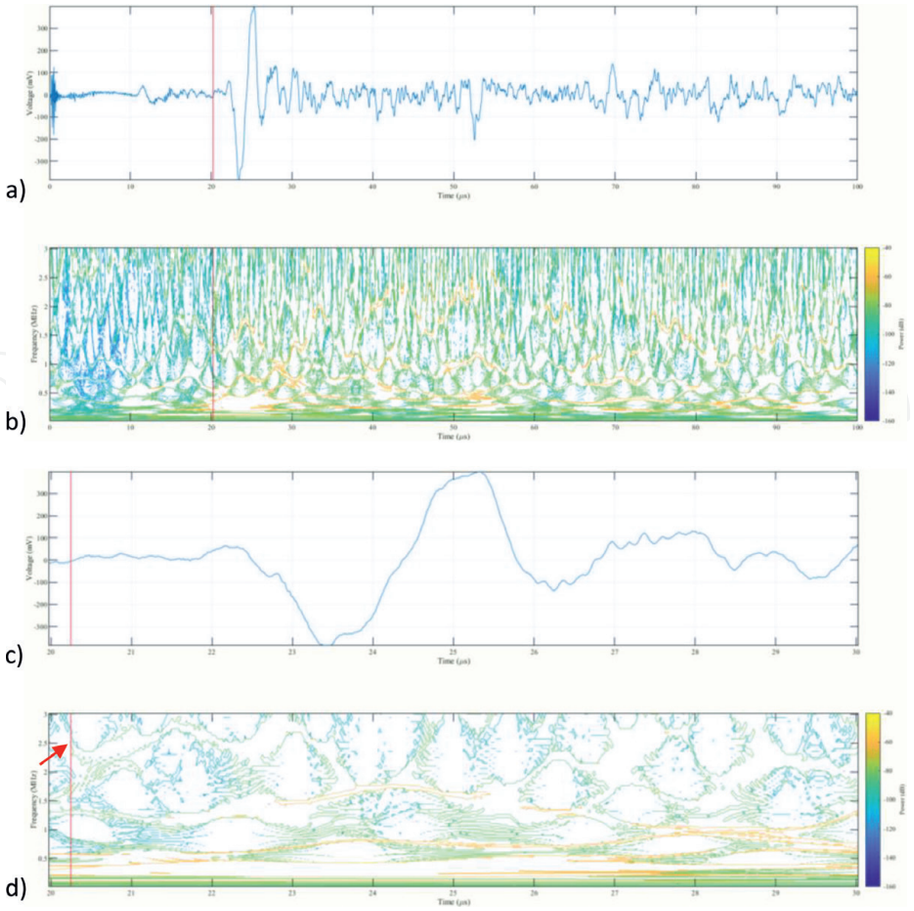

Figure 11.
Synchrosqueezing wavelet transform contour map of the scan point 3. (a) Time-based signal. (b) Synchrosqueezing transform contour map. (c) Detail of the time-based signal. (d) Detail of the synchrosqueezing transform contour map with an initial presence of acoustic activity at 20.244 μs, 2.57 MHz @−89.64 dB.

Wavelet	Scan point 1	Scan point 2	Scan point 3
Morlet	20.22	18.58	18.28
Mexican hat	23.05	19.98	20.98
Db4	21.65	18.95	18.50

Table 2.
Resulting time of flight from the internal defect in microseconds.

Wavelet	Scan point 1	Scan point 2	Scan point 3
Morlet	0.57	0.28	1.18
Mexican hat	3.40	1.68	3.88
Db4	2.00	0.65	1.40

Table 3.
Resulting time of flight error compared with the true time of flight, in microseconds.

	Scan point 1	Scan point 2	Scan point 3
Synchrosqueezing transform	21.08	23.56	20.24

Table 4.
Resulting time of flight from the internal defect in microseconds.

	Scan point 1	Scan point 2	Scan point 3
Synchrosqueezing transform	1.43	5.26	3.14

Table 5.
Resulting time of flight error compared with the true time of flight, in microseconds.

for **Figure 6a–c**, respectively. **Figure 7** and **Figure 8** represent the same wavelet echo analysis for Mexican hat and db4 mother wavelets respectively. **Table 2** show the resulting TOF from the internal defects at three scan points with reference to the different mother wavelets while **Table 3** shows the error of the resulting TOF compared to the calculated true TOF for each of the cases in (**Table 2**). It is found that the use of the Morlet mother wavelet gives the least estimation error and it is apparently the most accurate mother wavelet to use for this kind of analysis.

For the case of the TFR that results from the application of the SSWT, it can be observed that by the accurate redistribution of the energy that compose to the signal, the obtained images achieve an improved depiction of their modal frequencies in comparison with the conventional CWT, aiding to superiorly identify the behavior of the phenomenon. Moreover, for the scope of application of this study, by identifying the first instant of time when the bi-dimensional manifold created by means of the contour mapping of the SSWT apparently becomes closed by connecting all the modal frequencies of the signal of interest, it is possible to determine the onset of said signal.

As is well known, the accurate determination of this instant of time is critical for the TOF-related methods; hence, by means of this methodology, the required precision for the onset pick is achieved when only the signal waveform is used for this purpose. Synchrosqueezing wavelet transform contour map for the scan points of interest and TOF estimation are calculated **Figures 9–11**. **Tables 4**–5. show the resulting TOF for the three scan points and Table 5 shows the corresponding error with comparison to the true TOF.

Nevertheless, considerations must be taken in order to not analyze a very small signal, this with the aim to avoid the negative effects of the Cone of Influence (COI) of the CWT, since the SSWT still leads to inaccuracies for these areas.

5. Conclusion

Indeed, the acoustic emission phenomena have been utilized as a powerful tool with the purpose to either detect, locate or assess damage for a wide range of applications. Derived from its monitoring, one of the major challenges in analyzing the resulting wavelet or synchrosqueezing transform signal is to identify and extract each generated AE event. Typically, this event detection is carried out by a thresholding approach over the raw signal. In this regard, the wavelet algorithm has resulted in a very useful and successful technique in detecting the time of flight of the acoustic emission echoes generated by defects at their corresponding frequencies. The accuracy of the algorithm was investigated experimentally using metallic structure. This algorithm is more powerful than the conventional Fourier transform algorithm. Various mother wavelets have been used to compare the correlation between the mother wavelet and the acquired A-scan signals. A mother wavelet with higher correlation would provide more accurate results. Thus, it is important to select the mother wavelet carefully to avoid misleading results. In regard with the synchrosqueezing transform, although improved resolution capabilities, the error in regard with the time of flight determination is not reduced. The Morlet wavelet is revealed as the most suitable wavelet dealing with such acoustic emission waves generated by means of LASER excitation.

Acknowledgements

This work was supported in part by the CONACyT scholarship grant number 411711, Mexico, and the Ministry of Economy and Competitiveness under the TRA2016-80472-R Research Project, Spain.

Conflict of interest

All authors declare that no conflict of interest exists at the time of manuscript submission.

Author details

Hossam Selim[1], Fernando Piñal Moctezuma[2], Miguel Delgado Prieto[2*], José Francisco Trull[1], Luis Romeral Martínez[2] and Crina Cojocaru[1]

1 Physics Department, Technical University of Catalonia, Terrassa, Barcelona, Spain

2 Electronics Engineering Department, Technical University of Catalonia, Terrassa, Barcelona, Spain

*Address all correspondence to: miguel.delgado@mcia.upc.edu

References

[1] Park JW, Yang IY, Im KH, Hsu DK, Song SJ, Kim HJ, et al. Nondestructive evaluation of rayleigh pitch-catch contact ultrasound waves on impacted-damaged composites. Materials Science Forum. 2008;**566**:267-272. DOI: 10.4028/www.scientific.net/MSF.566.267

[2] Li J, Zhang H, Ni C, Shen Z. Analysis of laser generated ultrasonic wave frequency characteristics induced by a partially closed surface-breaking crack. Applied Optics. 2013;**52**:4179-4185. DOI: 10.1364/AO.52.004179

[3] Tiwari KA, Raisutis R, Samaitis V. Hybrid signal processing technique to improve the defect estimation in ultrasonic non-destructive testing of composite structures. Sensors. 2017;**17**(12):2858. DOI: 10.3390/s17122858

[4] Everton SK, Dickens P, Tuck C, Dutton B. Identification of sub-surface defects in parts produced by additive manufacturing, using laser generated ultrasound. In Materials Science & Technology Conference and Exhibition. 2016;**1**:141-148

[5] Shan Q, Dewhurst RJ. Surface-breaking fatigue crack detection using laser ultrasound. Applied Physics Letters. 1993;**62**:2649-2651. DOI: 10.1063/1.109274

[6] Kreis T. Application of digital holography for nondestructive testing and metrology: A review. IEEE Transactions on Industrial Informatics. 2016;**12**:240-247. DOI: 10.1109/TII.2015.2482900

[7] Zhao Y, Ma J, Liu S, Guo R, Song J, Qing Z. Laser ultrasonic technique applied to inspect fatigue crack. In: FENDT 2013–Proceedings of 2013 Far East Forum on Nondestructive Evaluation/Testing: New Technology and Application; 2013. pp. 205-8. DOI:10.1109/FENDT.2013.6635557

[8] Erdahl DS, Ume IC. Online-offline laser ultrasonic quality inspection tool for multilayer ceramic capacitors–Part I. IEEE Transactions on Advanced Packaging. 2004;**27**:647-653. DOI: 10.1109/TADVP.2004.831823

[9] Zhang Y, Yang LU, Fan J. Study on feature extraction and classification of ultrasonic flaw signals. Wseas Transactions on Mathematics. 2010;**9**:529-538

[10] Dixon S, Burrows SE, Dutton B, Fan Y. Detection of cracks in metal sheets using pulsed laser generated ultrasound and EMAT detection. Ultrasonics. 2011;**51**:7-16. DOI: 10.1016/j.ultras.2010.05.002

[11] Lee K, Estivill-Castro V. Feature extraction and gating techniques for ultrasonic shaft signal classification. Journal Applied Soft Computing. 2007. DOI: 10.1016/j.asoc.2005.05.003

[12] Zhang P, Ying CF, Shen J. Directivity patterns of laser thermoelastically generated ultrasound in metal with consideration of thermal conductivity. Ultrasonics. 1997;**35**:233-240. DOI: 10.1016/S0041-624X(96)00106-0

[13] Gómez M, Castejón C, García-Prada J. Review of recent advances in the application of the wavelet transform to diagnose cracked rotors. Algorithms. 2016;**9**:19. DOI: 10.3390/a9010019

[14] Choi J, Hong JW. Characterization of wavelet coefficients for ultrasonic signals. Journal of Applied Physics. 2010;**107**. DOI: 10.1063/1.3429087

[15] Gao RX, Yan R. Wavelets: Theory and Applications for Manufacturing. US: Springer; 2011. DOI:

10.1007/978-1-4419-1545-0. https://doi.org/10.1007/978-1-4419-1545-0

[16] Abbate A, Frankel J, Das P. Wavelet Transform Signal Processing Applied to Ultrasonics. In: Thompson D.O., Chimenti D.E. (eds) Review of Progress in Quantitative Nondestructive Evaluation. Boston, MA : Springer. 1996. https://doi.org/10.1007/978-1-4613-0383-1_97

[17] Gabor D. Theory of communication * part 1. The analysis of information. Journal of the Institution of Electrical Engineers–Part III: Radio and Communication Engineering. 1945;**93**:429-457. DOI: 10.1049/ji-3-2.1946.0074

[18] Daubechies I, Lu J, Wu H-T. Synchrosqueezed wavelet transforms: An empirical mode decomposition-like tool. Applied and Computational Harmonic Analysis. 2011;**30**:243-261. DOI: 10.1016/j.acha.2010.08.002

[19] Li C, Liang M. Time–frequency signal analysis for gearbox fault diagnosis using a generalized synchrosqueezing transform. Mechanical Systems and Signal Processing. 2012;**26**:205-217. DOI: 10.1016/j.ymssp.2011.07.001

[20] Wang Z, Ren W, Liu J. A synchrosqueezed wavelet transform enhanced by extended analytical mode decomposition method for dynamic signal reconstruction. Journal of Sound and Vibration. 2013;**332**:6016-6028. DOI: 10.1016/j.jsv.2013.04.026

[21] Thakur G, Wu H. Synchrosqueezing-based recovery of instantaneous frequency from nonuniform samples. SIAM Journal on Mathematical Analysis. 2011;**43**: 2078-2095. DOI: 10.1137/100798818

[22] Jiang Q, Suter BW. Instantaneous frequency estimation based on synchrosqueezing wavelet transform. Signal Processing. 2017;**138**:167-181. DOI: 10.1016/j.sigpro.2017.03.007

[23] Thakur G, Brevdo E, Fučkar NS, Wu H-T. The Synchrosqueezing algorithm for time-varying spectral analysis: Robustness properties and new paleoclimate applications. Signal Processing. 2013;**93**:1079-1094. DOI: 10.1016/j.sigpro.2012.11.029

[24] Selim H, Delgado Prieto M, Trull J, Romeral L, Cojocaru C. Laser Ultrasound Inspection Based on Wavelet Transform and Data Clustering for Defect Estimation in Metallic Samples. Sensors. 2019;**19**:573. DOI: 10.3390/s19030573